Using Open-Path Dual-Comb Spectroscopy to Monitor Methane Emissions from Simulated Grazing Cattle

Chinthaka Weerasekara,[1] Lindsay C. Morris,[2] Nathan A. Malarich[3], Fabrizio R. Giorgetta,[3,4] Daniel I. Herman, [3,4] Kevin C. Cossel,[3] Nathan R. Newbury,[3] Clenton E. Owensby,[1] Stephen M. Welch,[1] Cosmin Blaga,[2] Brett D. DePaola,[2] Ian Coddington,[3] Eduardo A. Santos,[1] and Brian R. Washburn[3]

[1]Kansas State University, Department of Agronomy, Manhattan, KS, 66506, United States
[2]Kansas State University, Department of Physics, Manhattan, KS, 66506, United States
[3]National Institute of Standards and Technology, Communications Technology Laboratory, Boulder, CO, 80305, United States
[4]University of Colorado, Boulder, Department of Physics, Boulder, CO, 80309, United States

Correspondence to: Brian R. Washburn (brian.washburn@nist.gov), Eduardo Santos (esantos@ksu.edu)

Abstract. Accurate whole-farm or herd-level measurements of livestock methane emissions are necessary for anthropogenic greenhouse gas inventories and to evaluate mitigation strategies. A controlled methane (CH_4) release experiment was performed to determine if dual comb spectroscopy (DCS) can detect CH_4 concentration enhancements produced by a typical herd of beef cattle in an extensive grazing system. Open-path DCS was used to measure downwind and upwind CH_4 concentrations from ten point-sources of methane simulating cattle emissions. The CH_4 mole fractions along with wind velocity data were used to calculate CH_4 flux using an inverse dispersion model, and the simulated fluxes were then compared to the actual CH_4 release rate. For a source located 60 m from the downwind path, the DCS system detected 10 nmol mol^{-1} CH_4 horizontal concentration gradient above the atmospheric background concentration with a precision of 6 nmol mol^{-1} in 15-min interval. A CH_4 release of 3970 g day^{-1} was performed resulting in an average concentration enhancement of 24 nmol mol^{-1} of CH_4. The calculated CH_4 flux was 4002 g day^{-1} with an error of ±1498 g day^{-1}. Periodically altering the downwind path, which may be needed to track moving cattle, did not adversely affect the ability to determine the CH_4 flux. These results give us confidence that CH_4 flux can be determined by grazing cattle with low disturbance and direct field-scale measurements.

1 Introduction and motivation

Methane (CH_4) emissions from enteric fermentation in domestic ruminants is the largest anthropogenic source of CH_4 in the United States, with the dairy and beef industries being responsible for most of these emissions (EPA, 2023). Previous life-cycle analyses indicate that 70 to 80% of the total greenhouse gas (GHG) emissions from the beef sector occur during the grazing phase (Alemu et al., 2017; Rotz et al., 2015; Thompson and Rowntree, 2020). However, direct herd-scale CH_4 emission data in grazing systems are scarce. The low animal density and high animal mobility commonly found in most grazing systems makes herd-scale measurements quite challenging (Dengel et al., 2011; Felber et al., 2015; Flesch et al., 2018; Laubach et al., 2016; Stoy et al., 2021). Accurate whole-farm and herd-level measurements of livestock methane emissions are necessary to

evaluate mitigation strategies to reduce GHG emissions, improve current GHG national inventories and to assist governments, industries, and other organizations to fulfil commitments to reduce anthropogenic GHG emissions.

Methane emissions from individual animals have been measured using face masks (Place et al., 2011), head-hood chambers (Hill et al., 2016), whole-animal respiration chambers (Pinares-Patiño et al., 2011), tunnels (Lockyer and Jarvis, 1995), automated spot head-box measurements (Hristov et al., 2015) and tracer methods (Grainger et al., 2007; Johnson et al., 1994). The respiration chamber is considered the standard technique for measuring livestock CH_4 emissions. Results from chamber studies have been used to develop predictive models and equations for national GHG inventories (Danielsson et al., 2017; Ramin and Huhtanen, 2013). However, chambers can create measurement artefacts by affecting animal behaviour and are not practical for measuring CH_4 emissions from many animals (Storm et al., 2012).

Micrometeorological techniques have been applied for measuring ammonia, carbon dioxide, nitrous oxide and CH_4 emissions from livestock systems (Laubach et al., 2024; McGinn and Flesch, 2018b; Phillips et al., 2007; Prajapati and Santos, 2018b; Sun et al., 2015), and have the advantages of being non-intrusive, can integrate fluxes from large areas or herds of cattle reducing measurement uncertainties due to animal-to-animal variability, and provide high temporal resolution (<1 h) flux measurements (McGinn, 2013). The widely used eddy covariance technique has been combined with flux footprint models to estimate methane emissions from ruminant herds (Coates et al., 2017; Dengel et al., 2011; Prajapati and Santos, 2018a; Stoy et al., 2021). However, this approach requires that the presence of animals in the flux tower footprint, which makes its implementation challenging in extensive grazing systems where cattle often do not remain for long periods in the area sampled by the flux tower.

Lagrangian stochastic models, which are the basis for several inverse dispersion models (IDM), have been used to infer emissions of gases such as ammonia and CH_4 from agricultural systems (Flesch et al., 2005; Laubach and Kelliher, 2005; McGinn and Flesch, 2018b). Unlikely traditional micrometeorological methods, such as the eddy covariance and flux gradient methods, they can handle source areas of different sizes and complex source geometries (Flesch et al., 2005). The IDM proposed by Flesch et al. (1995) has been used to quantify CH_4 emissions from ruminants (Flesch et al., 2018; Laubach and Kelliher, 2005; McGinn et al., 2011; Prajapati and Santos, 2018a). In typical IDM applications, open-path line-averaged concentration sensors are placed upwind and downwind from the source of interest. The gas emission rates are then inferred based on the increase of gas concentration downwind from the source and turbulence statistics obtained from wind velocity measurements. McGinn et al. (2011) used IDM to estimate methane emissions from 18 animals grazing in a 1-ha paddock. They measured the area with five different paths ranging from 80 m to 128 m in length, so that at least one laser path was close enough to the cattle for their open-path system to be able to detect an enhancement in concentration. The main goal of this study is to determine if the dual-comb spectroscopy (DCS) combined with an IDM can precisely infer CH_4 flux from a typical herd of cattle grazing on an extensive pasture.

2 Methods

22.1 Dual comb spectroscopy

Formatted: Heading 2

Dual-comb spectroscopy is a spectroscopic technique that uses two coherent frequency combs to get molecular concentrations through absorption (Coddington et al., 2016). A frequency comb is a laser spectrum composed of many (10^6) regularly spaced (MHz) spectral lines known as comb teeth with spectral coverage of multiple THz. Two frequency combs with slightly different repetition rates pass through a gas. Atmospheric molecular absorption lines, such as those due to CH_4, have GHz-wide absorption features and will absorb multiple comb teeth. After passing through the gas, the light from the combs is incident onto a square-law photodetector generating a radio frequency (RF) comb composed of heterodyne beats between pairs of optical comb teeth. From this an electrical interferogram (IGM) is generated, and its Fourier transform provides both the gas absorption and laser spectra. DCS is a sensing tool that combines and enhances the most desirable traits of FTIR and tunable diode laser absorption spectroscopy to measure entire absorption bands of multiple gas species at high speed with fine spectral resolution. In particular, DCS offers the unique ability to interrogate kilometer-scale paths and reliably measure very small changes in gas concentration making DCS potentially valuable for quantifying fluxes of agriculturally significant gases in the field scale.

2.2 Obtaining CH_4 mole fractions using spectral line fitting

Formatted: Subscript

Formatted: Heading 2

DCS is commonly used in an open-path differential measurement geometry to measure gas mole fraction on two beam paths to determine CH_4 flux from a source area. As seen in Fig. 1a, comb light generated from the DCS system in a trailer is split and sent on upwind and downwind paths. A sample IGM (Fig. 1b), from each path is recorded and its Fourier transform provides both the gas absorption and laser spectra (Fig. 1c). In order to obtain gas mole fraction, the spectral absorption is fit using a nonlinear curve fitting routine (Newville et al., 2014) using molecular information from the HITRAN spectral database (Gordon et al., 2017; Rothman et al., 2009). The open-path DCS system used for this study has spectral coverage from 179.8 THz to 188.9 THz (6000 cm^{-1} to 6300 cm^{-1}) and with a spectral resolution of 200.005 MHz (0.00667 cm^{-1}). The system is designed to target CH_4, CO_2, and water vapor with laboratory-level precision while operating in the field. It is based on all-polarization-maintaining, mode-locked erbium-doped fiber lasers with repetition frequencies 200,005,000 Hz and 200,005,000 + 208.88 Hz respectively (Sinclair et al., 2015). Mutual comb coherence is established by phase-locking each comb to the same free-running continuous wave laser at 192.175 THz and by phase-locking the carrier-envelope offset frequency of each comb using an in-line *f*-to-2*f* interferometer (Truong et al., 2016). To tailor the comb spectrum to cover the CH_4 absorption band at 181.97 THz, light for each comb is amplified in an erbium-doped fiber amplifier and sent through a short piece of highly nonlinear fiber. For the DCS measurement, the filtered outputs are combined using a fiber combiner generating two outputs that are directed over two open-air paths.

Each IGM is digitally sampled with 14 bits and contains 957500 points. The IGMs are generated at a rate of 208.88 Hz, so streaming and storing these data to a computer would require terabits of storage. To reduce data storage

requirements, during the course of the measurement, 28 IGMs are co-added by a field programmable gate array (FPGA) to produce a hardware-averaged IGM. These IGMs are streamed to a computer, which performs phase-correction and additional averaging using methodology similar to techniques used in FTIR (Griffiths and de Haseth, 2006). The computer calculates a phase-corrected IGM every 5 min and stores it in the hard drive. For the best case, 2238 hardware-averaged IGMs are used to generate a phase-corrected IGM every 5 min. Hardware-averaged IGMs with poor return power, mostly due to poor alignment between transceiver and the retroreflector, are rejected and not used in the phase-correction. Under moderate windy conditions IGM rejection is less than 10%.

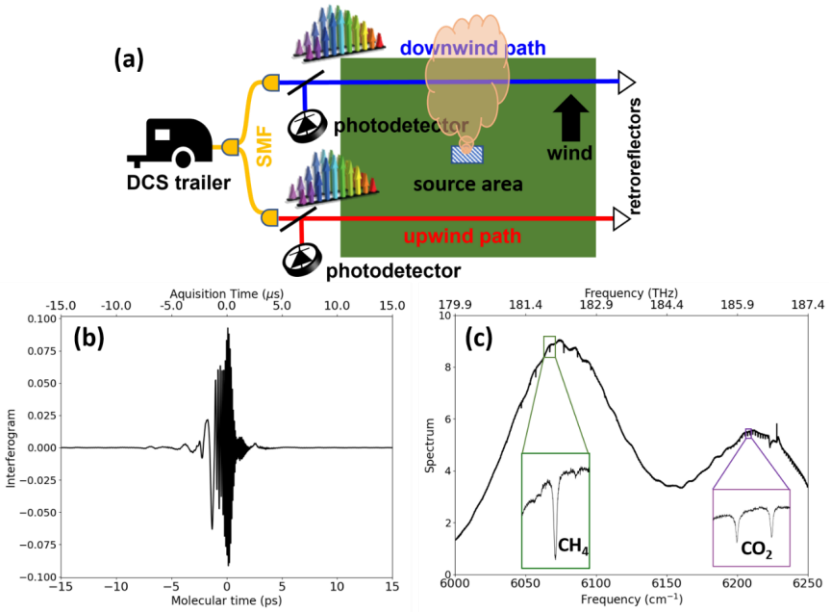

Figure 1: (a) Schematic of the dual-comb spectrometer gas concentration measurements on two paths from a CH_4 source area. Yellow lines indicate single-mode fiber (SMF) transmitting dual-comb light to an upwind (red) and downwind (blue) open-air paths. CH_4 is emitted from an area between the two paths under proper wind directions. RF signals from two photodetectors are sent back to the trailer and two interferograms (IGM) containing gas concentration information for each path are digitized. (b) A dual-comb spectroscopy phase-corrected IGM after 5 min acquisition time on the upwind path. 'Acquisition time' is the microsecond timescale of the measured RF voltage. 'Molecular time' is the timescale associated with the period of molecular oscillations which is typically picoseconds. (c) The Fourier transform of the IGM with insets showing CH_4 and CO_2 absorption lines and the laser baseline.

2.3 ~~Langrangian~~Lagrangian stochastic model (WindTrax) simulations

2.3.1 Sensitivity and precision required for grazing measurements

~~3 Sensitivity and precision required for grazing measurements~~

A forward Lagrangian stochastic model (Windtrax, Thunderbeach Sci.; Crenna, 2006) was used to simulate the concentration field downwind from a hypothetical herd of 20 head of beef cattle grazing in an area of 25 ha, which is a typical stocking density (animal/area) in the Flint Hills region, Kansas (Fig. 2). Wind orthogonal components and temperature data were measured at 10 Hz using a sonic anemometer (CSAT3, Campbell Sci, Logan, UT) deployed 5 m above a grazing unit on the Rannells' Flint Hills Prairie Preserve (full site description below) near Manhattan, Kansas USA. The wind dataset selected for these simulations consisted of about 30 days in June, 2021 during the grazing season. The wind raw data files were processed using the software Eddy Pro (Licor, Lincoln, NE) and means, variances and covariances for wind velocity and sonic temperature data were calculated for 30-min intervals to be used as input variables for the WindTrax simulations. To investigate if the DCS system can resolve the expected increase in CH_4 concentration due to the presence of cattle above the typical CH_4 atmospheric background level (2000 nmol mol-1), two expected CH_4 emission scenarios were evaluated: 100 g $head^{-1}$ day^{-1} and 300 g $head^{-1}$ day^{-1}. These values were selected based on the reported IPCC Tier 1 emission values for grazing cattle in North America of 208 g $head^{-1}$ day^{-1} (Eggleston et al., 2006). The simulated herd consisted of a fixed grid of point sources spaced 20 meters apart (Fig. 2). The height of gas release was set to 1 meter above the ground to mimic the height of the animal mouth and a total of 50,000 particles were released for each point source. Three beam lines were used in this simulation located at 45, 160 and 310 m from the geometric center of the herd.

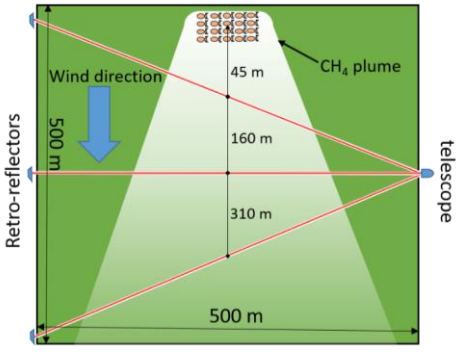

Formatted: Heading 2

Formatted: Subscript

Formatted: Subscript

Formatted: Subscript

Formatted: Superscript

Formatted: Superscript

Formatted: Superscript

Formatted: Superscript

Formatted: Superscript

Formatted: Superscript

Figure 2: Schematic diagram showing the location of the hypothetical herd of cattle, transceiver, retroreflectors and three possible downwind paths used for the forward WindTrax simulations. A constant background of 2000 nmol/mol was assumed so no upwind path was used in the simulation and not shown in the figure.

The forward model predicted that a herd of 20 cattle grazing in an area of 25 ha would produce a CH_4 enhancement of 16 nmol mol^{-1} above a 2000 nmol mol^{-1} background for a beamline 45 m away from the herd of cattle assuming an emission rate of 300 g head^{-1} day^{-1} of CH_4. The enhancement drops to 2 nmol mol^{-1} for a beam path 310 m away assuming the same emission rate. For a low emission scenario (100 g head^{-1} day^{-1}), the CH_4 enhancements ranged from 5 to 1 nmol mol^{-1} for a beam line located at 45 m and 310 m away from the center of the herd.

Table 1 - Grazing system methane emission WindTrax simulation results showing the expected average and standard deviation (SD) of CH_4 concentration measured by line sensors positioned downwind from a cattle herd with two CH_4 emission rates. The CH_4 background level was assumed to be constant at 2000 nmol mol^{-1}.

	Cattle CH_4 emission rate (g head^{-1} day^{-1})					
	100			300		
Distance (m)	45	160	310	45	160	310
[CH_4] (nmol mol^{-1})	2005	2002	2001	2016	2006	2002
SD [CH_4] (nmol mol^{-1})	12	4	2	36	12	7

Figure 3(a) shows spectral data and the results of a H_2O, CH_4, and CO_2 fit. The DCS concentration measurement precision under field conditions was determined using Allen-Werle analysis (Werle, 2011) which includes effects of field-condition induced misalignment to the retroreflectors which causes fluctuations in the signal-to-noise ratio (SNR). The result of an Allen-Werle analysis on a dataset taken for 24 hours on 18 Dec 2022 is shown in (Fig. 3b), showing a precision of 6 nmol mol^{-1} CH_4 in 900 s (15 min) for 200-m paths. This result is consistent with results of (Herman et al., 2021) where data were taken with a SNR of 1000 and a precision of 25 nmol mol^{-1} in 5 min.

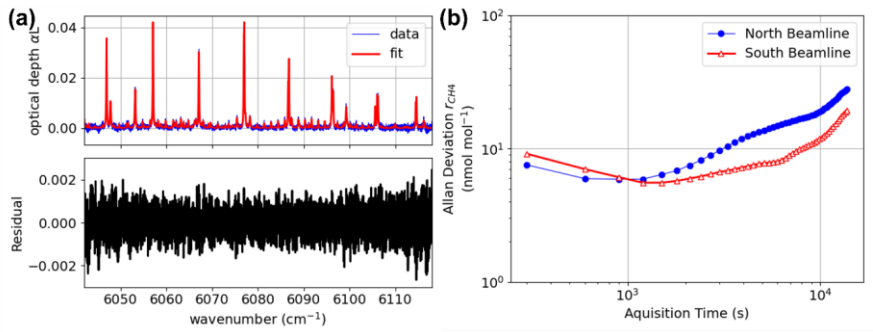

Figure 3: (a) Result of cepstral-domain fitting of H_2O, CH_4, and CO_2 for 300 s averaged data, showing the resulting optical depth data, fit, and fit residual. (b) Allan-Werle deviation of the CH_4 dry mole fraction (r_{CH4}) showing 6 nmol mol^{-1} precision in 900 s.

2.3.2 Computing CH_4 flux using an inverse dispersion model

Formatted: Heading 3

~~A freely available IDM software, WindTrax (Crenna, 2006),~~ ~~Windtrax~~WindTrax was also ~~was~~ used for computing CH_4 fluxes using. ~~The WindTrax input data consisted of measured~~ upwind and downwind CH_4 dry mole fractions (Section 3.1), and ~~mean, variance and covariances of wind velocity and temperature, obtained using the sonic anemometer data~~ wind velocity data as described in section 2.3.1. As WindTrax flux estimates are more precise for 15 minute or longer timescales (Flesch et al., 2004), we averaged the 5-min DCS mole fraction data to 15-min. WindTrax requires appropriate weather conditions to provide accurate estimate of fluxes, so the data were screened based on the following acceptance criteria: wind friction velocity (u^*) > 0.1 m s^{-1} and absolute Monin-Obukhov Length values $|L_{MO}|$ > 10 m- (Flesch et al., 2005; Todd et al., 2014). The source area (Fig. 4) used by WindTrax to infer fluxes was set to match the 12.5 m^2 area of the CH_4 point sources and the source level was set to 0.7 m above the ground which is the same heigh as the manifold outlets. In WindTrax all DCS measurement paths were modelled as line concentration sensors consisting of 60 particle "release" points along the path, starting at the transceiver and ending at the retroreflector. A total of 50,000 particles were released from each of those points for each WinTrax simulation.

One of the principal sources of uncertainty in the IDM estimates arises from the errors in the gas concentration measurements themselves. The flux is dependent on the difference between downwind (r_d) and upwind (r_u) dry mole fractions, measured the north and south beamlines (Fig. 4). The fractional uncertainty in the flux is given by (Herman et al., 2021):

$$\frac{\sigma_F}{F} = \frac{\sqrt{\sigma_{r_d}^2 + \sigma_{r_u}^2 - 2cov(r_d, r_u)}}{r_d - r_u} \quad (2)$$

where F is the flux, σ_F is flux error, $\sigma^2_{r_d}$ is downwind (background) dry mole fraction error, $\sigma^2_{r_u}$ is upwind dry mole fraction, *cov(d,u)* is the covariance of the downwind and upwind errors. A covariance term was added to the quadrature error following previous studies (Bai et al., 2022; Herman et al., 2021) to account for small correlations in the different path errors. The errors in the dry mole fractions ($\sigma^2_{r_d}$ and $\sigma^2_{r_{ud}}$) and the covariance were determined from the recorded 5-min measured SNR assuming that the mole fraction error is inversely proportional to the SNR. The fractional uncertainty ignores errors due to measurement deadtime, wind field measurements and IDM inherent uncertainties (Flesch et al., 2004). Typical values fractional uncertainty in the flux varies from 20 to 30%.

Formatted: Indent: First line: 0"

3 Controlled CH_4 release experiment

3.1 Description

Formatted: Heading 2

Controlled CH_4 release field experiments were conducted on the Rannells' Flint Hills Prairie Preserve (hereafter Rannells' ranch) near Manhattan, Kansas USA (39º 08' 28''N, 96º 31' 31''W, 324 m asl). The dominant steer grazing system in the Kansas Flint Hills is Intensive Early Stocking (IES) (Smith and Owensby, 1978). IES is a grazing system that takes advantage of the early summer high quality forage by stocking at twice the normal season-long stocking rate (1.25 steers/ha) for the first half of the growing season (~May 1 to ~July 15) with no grazing during the last half. The grazing unit used in the study has 31 hectares and has been annually burned in late April each year. This grazing unit was selected because its topography is suitable for micrometeorological measurements and because it allows unobstructed paths for the DCS system for most of its extension.

Previous work (Alden et al., 2019; Coburn et al., 2018) used DCS to measure simulated CH_4 leaks from oil and gas production at the level of 1400 g day^{-1} from a distance of 1 km. Here we seek to provide a similar verification of the technology but with two important changes in the measurement configuration appropriate for livestock-based methane sources. First, the sources will be distributed rather than concentrated to single point source, ~~S~~secondly the sources are further from the measurement paths. This larger separation will be necessary to accommodate the fact the herd will wander over time. The measurement paths might be adjusted to accommodate the cattle movement but there will be a limit to how close the measurement paths can be kept from the source.

The DCS system was housed in a temperature-controlled trailer at the Rannells' Ranch as seen in Fig. 4. Single-mode telecommunication fibers (Corning SMF-28) of lengths 10 and 40 m carried the dual-comb laser output light to two telescope transceivers (Fig. 4b) that were used to send comb light across the North (blue) and South (red) beamlines. The transceiver consisted of an FC/APC fiber termination followed by a collimating 179 mm focal length, 102 mm diameter, 45° off-axis parabolic mirror resulting in a collimated beam of ~35 mm diameter. Eye-safe (<10 mW) collimated dual-comb light was

directed with a 127 mm clear aperture, 5 arcsec gold retroreflector (Edmund Optics†) positioned 200 m away (Fig. 4a) and the reflected signal was focused onto a 150-MHz bandwidth photodetector (PDA10CF, Thorlabs, Newton, NJ) in the transceivers. RF signals from photodetectors were transmitted to the trailer through RF cables (RG58, Pasternack Irvine, CA) and digitized using a 14-bit digitizer (FMC104, Abaco Systems, Huntsville, AL). To remove any concentration bias due to digitizer nonlinearities we added a dither signal to the received DCS interferogram (Malarich et al., 2023). The dither improved the individual channel precision by 5% and reduced the differences between channels to below 3 nmol mol^{-1}.

Both transceivers were mounted on motorized tip/tilt gimbals (PT100, FLIR, Wilsonville, OR) that were automatically aligned using a datalogger (CR1000x, Campbell Sci.) or personal computer algorithms to the retroreflectors based on the return DC signal from the photodetector. The transceiver also housed a visible camera (BFLY-PGE-50A2M-CS, FLIR) to aid with alignment and a consumer 5W 850-nm LED flashlight to allow the user to see the retroreflectors with the visible camera during nighttime. The datalogger-controlled alignment system was able to maintain sufficient power back from the retroreflector to the transceiver in moderate wind conditions for over 24 hours. The wind velocity orthogonal components and temperature were measured using a sonic anemometer (CSAT3 Campbell Sci.) at 5 m above the ground. The sonic anemometer was connected to a datalogger (CR3000, ~~Camppell~~Campbell Sci.) and the raw data were saved at 10 Hz. The positions of retroreflectors, manifold, sonic anemometer and transceiver were measured using a multi-band real-time kinematic positioning (RTK) receiver (Reach RS2+, Emlid, Budapest, Hungary) with 7 mm and 14 mm horizontal and vertical accuracies, respectively. The horizontal and vertical coordinates obtained for the transceivers and retroreflectors were then used to determine the path lengths shown in Fig. 4.

A custom-built gas manifold (Fig. 4c) was used to control the release of CH_4 through 10 point sources located within the two DCS beam lines. Methane gas from a compressed tank (99.97% purity) was delivered to a proportional solenoid valve (PVQ13, SMC, Noblesville, IN) using a two-stage pressure regulator and high-density polyethylene tubing (I.D. 5.3 mm). The proportional valve was then connected to a multi-port aluminium manifold using high density polyethylene tubing. The pressure inside the manifold was monitored using a pressure transducer (PX119-030GI, Omega, Norwaok, CT). The CH_4 from the manifold flowed through ten 0.254-mm precision orifice assemblies (K2-10-SS, O'Keefe Controls Co., Monroe, CT). The precision orifice assemblies were then connected to 8-m high density polyethylene tubing lengths. The other extremity of these plastic tubes was then attached to metal rods at a height of 0.7 m above the ground. During CH_4 controlled-release campaigns, the pressure inside the manifold was adjusted to provide the desired flow rate by controlling the voltage applied to the proportional valve using a datalogger (CR1000, Campbell Sci.). A feedback loop between proportional valve and pressure transducer ensured a constant pressure inside the manifold during the control release campaigns. The CH_4 tank was weighted in the beginning and end of the gas release campaigns and the mass of gas released was determined gravimetrically using a

† Certain equipment or instruments are identified in this paper in order to specify the experimental procedure adequately. Such identification is not intended to imply recommendation or endorsement of any product by NIST, nor is it intended to imply that the equipment identified are necessarily the best available for the purpose.

scale (D125WQL, Ohaus, Parsippany, NJ). We used the mass given by the scale to determine the amount of gas released in each release campaign since it provides a more direct estimate of the release rate than the one obtained using the gas manifold. Previous gas release study has successfully used scale data to verify the flow rate of mass flow controller (Coates et al., 2017).

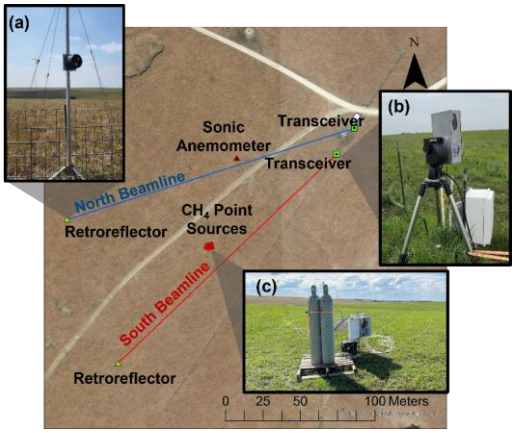

Figure 4: Layout of the experimental site the Rannells' Flint Hills Prairie Preserve. Insets: (a) hollow gold retroreflectors, (b) optical transceiver on a tip/tilt gimbal, and (c) gas manifold and point sources used to release CH_4 at a known rate. The one-way path distances were 202 m for the North Beamline and 203 m for the South Beamline.

~~5 Obtaining CH_4 mole fractions using spectral line fitting~~

Mole fractions (χ) of CO_2, H_2O, and CH_4 were obtained from the measured interferogram using a fit model derived from a combination of the HITRAN databases (Rothman et al., 2013) and the cepstral-domain technique (Cole et al., 2019). Temperature and pressure data used as an initial guess for the fit were provided by the sonic anemometer (CSAT3) and a pressure transducer (CS100, Campbell Sci.), respectively, which were both located on the same tower during the measurement campaign. The spectral band used in the cepstral-domain fitting was from 6000 cm^{-1} to 6300 cm^{-1} and contains CH_4, H_2O as well as weak CO_2 absorption lines. HITRAN 2008 (Rothman et al., 2009) molecular parameters for CH_4 with a Voigt lineshape computed using the HITRAN Application Programming Interface (Kochanov et al., 2016). Line-strengths greater than 10^{-22} cm^{-1} $molecule^{-1}$ cm^2 were used. A cepstral-domain filter operates in the time domain and removes broad comb baseline structure in the IGM at times shorter than 15 ps and removes an etalon feature from 30 to 40 ps. The conversion from CH_4 mole fraction (χ_{CH4}) to dry mole fraction (r_{CH4}) was calculated using the fit H_2O mole fraction (χ_{H2O}) and

$$r_{CH4} = \frac{\chi_{CH4}}{1-\chi_{H2O}} \quad (1)$$

6 Computing CH_4 flux using an inverse dispersion model

A freely available IDM software, WindTrax (Crenna, 2006), was used for computing CH_4 fluxes. The WindTrax input data consisted of measured upwind and downwind CH_4 dry mole fractions, and mean, variance and covariances of wind velocity and temperature, obtained using the sonic anemometer data. As WindTrax flux estimates are more precise for 15 minute or longer timescales (Flesch et al., 2004), we averaged the 5-min DCS mole fraction data to 15-min. WindTrax requires appropriate weather conditions to provide accurate estimate of fluxes, so the data were screened based on the following acceptance criteria: wind friction velocity (u^*) > 0.1 m s^{-1} and absolute Monin-Obukhov Length values $|L_{MO}|$ > 10 m (Flesch et al., 2005; Todd et al., 2014). The source area (Fig. 4) used by WindTrax to infer fluxes was set to match the 12.5 m^2 area of the CH_4 point sources and the source level was set to 0.7 m above the ground which is the same heigh as the manifold outlets. In WindTrax all DCS measurement paths were modelled as line concentration sensors consisting of 60 particle "release" points along the path, starting at the transceiver and ending at the retroreflector.

One of the principal sources of uncertainty in the IDM estimates arises from the errors in the gas concentration measurements themselves. The flux is dependent on the difference between downwind (r_d) and upwind (r_u) dry mole fractions, measured the north and south beamlines (Fig. 4). The fractional uncertainty in the flux is given by (Herman et al., 2021):

$$\frac{\sigma_F}{F} = \frac{\sqrt{\sigma_{r_d}^2 + \sigma_{r_u}^2 - 2cov(r_d, r_u)}}{r_d - r_u} \quad (2)$$

where F is the flux, σ_F is flux error, $\sigma_{r_d}^2$ is downwind (background) dry mole fraction error, $\sigma_{r_u}^2$ is upwind dry mole fraction, $cov(d,u)$ is the covariance of the downwind and upwind errors. A covariance term was added to the quadrature error following previous studies (Bai et al., 2022; Herman et al., 2021) to account for small correlations in the different path errors. The errors in the dry mole fractions ($\sigma_{r_d}^2$ and $\sigma_{r_u}^2$) and the covariance were determined from the recorded 5-min measured SNR assuming that the mole fraction error is inversely proportional to the SNR. The fractional uncertainty ignores errors due to measurement deadtime, wind field measurements and IDM inherent uncertainties (Flesch et al., 2004). Typical values fractional uncertainty in the flux varies from 20 to 30%.

73.2 Results from controlled CH_4 release measurements

Formatted: Heading 2

Data from a CH_4 release at a rate of 3078 g day-1 equivalent to 15 head of grazing cattle is shown in Fig. 5. The wind speed showed high variability reaching with minimum and maximum values equal to 0.7 and 7.6 m/s, respectively (Fig. 5a). CH_4 mole fraction was measured at 5-min intervals for the North and South laser beamlines as seen in Fig. 4. The CH_4 gas release started at 10:30 and ended at 18:00 on 04 Feb 2023. The enhancement is given by $r_d - r_u$ (Fig. 5c). The small 10 nmol mol^{-1} average enhancement can be seen fluctuating around a 2026 nmol mol^{-1} average background concentration. However, the wind speed affected the DCS ability to measure these small concentration enhancements by diluting the methane plume as can be

seen when the wind speed values were high during the afternoon of 04-Feb-2023. The two-path DCS measurement was also capable of capturing the temporal dynamics of the CH_4 background driven by changes in atmospheric boundary layer conditions.

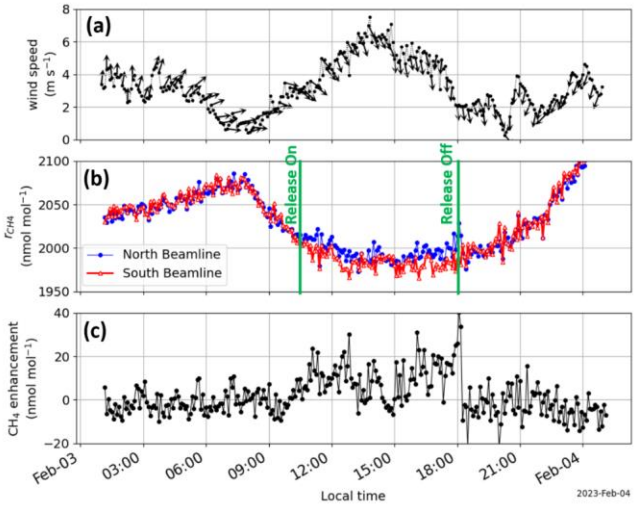

Figure 5: 5-min values of (a) wind speed and direction, (b) dry CH_4 mole fraction (r_{CH4}), and (c) enhancement during a controlled CH_4 release of 3078 g d^{-1} equivalent to 15 head of cattle assuming a CH_4 rate of 208 g $head^{-1}$ day^{-1}. Wind arrows point in the direction from which the wind is blowing. During the release, wind was mostly from the south causing an enhancement on the North Beamline.

We used downwind and upwind DCS concentration measurements for a period with no gas release to determine if any concentration biases exist between the North and South beamlines that may lead to incorrect flux values and to estimate the precision of CH_4 fluxes inferred using DCS and WindTrax. North and south measurements were taken over 6.25 hours with no gas released with the wind from the west (Fig. 6). CH_4 dry mole fraction and WindTrax were used to compute an average CH_4 flux of 1.3 g day^{-1} and standard deviation of ± 217.5 g day^{-1}. This standard deviation value is equivalent to approximately one head of cattle, assuming an emission rate of 200 g $head^{-1}$ day^{-1}.

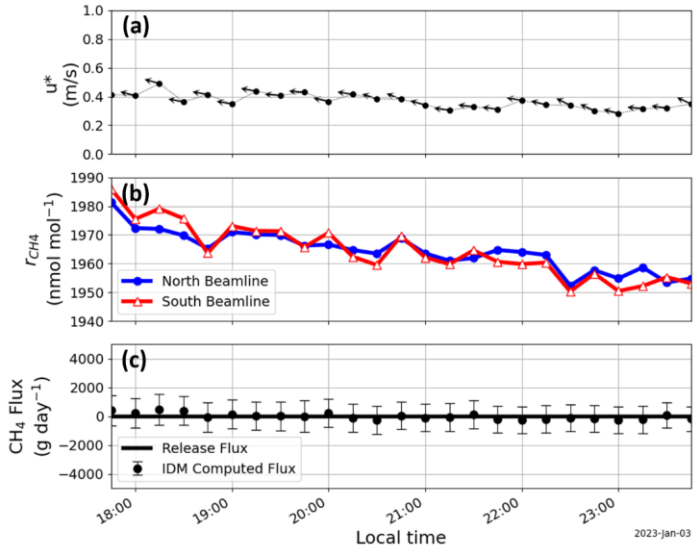

Figure 6: Time series of (a) wind friction velocity and direction, (b) dry CH_4 mole fraction (r_{CH4}), and (c) release and IDM computed CH_4 flux a case of no released gas. The error bars are uncertainties due to the DCS measured concentrations calculated using Eq. 2. Wind arrows point in the direction from which the wind is blowing.

To test if the DCS measurement can be used correctly reproduce the release flux rate, a controlled CH_4 release corresponding to 3970 g day^{-1}, which simulates a 19-head cattle herd with emission rate of 200 g head^{-1} day^{-1}, was performed where DCS measured concentrations and 3D wind statistics was measured for six hours (Fig. 7). DCS dry mole fractions and wind data for 15-min intervals were then used to estimate CH_4 fluxes using WindTrax. The DCS system was able to detect the small 24 nmol mol^{-1} average enhancement above the 2041 nmol mol^{-1} average background concentration. WindTrax computed average CH_4 flux was 4002 g day^{-1} and the flux uncertainty due to DCS concentration errors (Eq. 2) ± 1498 g day^{-1}, showing a good agreement to the actual release CH_4 flux of 3970 g day^{-1}. As a point of comparison Harper *et al*. (2010) summarized the accuracy of IDM in 13 controlled release studies. They expressed the IDM accuracy by a recovered rate, given by ($F_{IDM}/F_{release}$)×100, finding an average recovery rate of 95% for all the studies. We estimated our recovery rate to be 100.8 (4002/3970 × 100) using the data shown in Fig. 7a. This is a noteworthy result indicating that the combination of DCS with IDM can produce flux estimates with high accuracy.

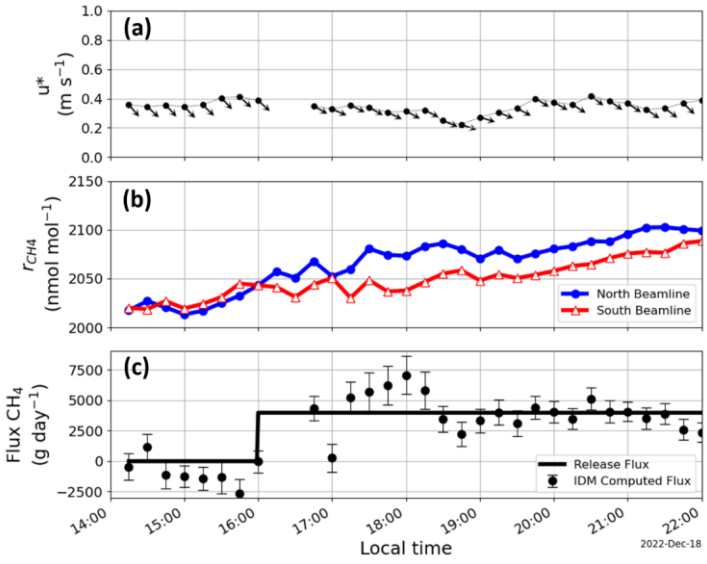

Figure 7: Timeseries of (a) wind friction velocity and direction, (b) CH_4 dry mole fraction (r_{CH4}), and (c) release and IDM computed CH_4 flux for a CH_4 release of 3970 g day^{-1} equivalent to 19 head of cattle. Wind arrows point in the direction from which the wind is blowing.

Monitoring grazing cattle emissions in the field will require changing between laser paths to capture emissions from a moving herd. To investigate the effect of the distance between the herd and the beam paths, we alternated between two downwind south paths (Fig. 8). Here a release simulating 40 head was performed where the downwind south path was changed at hour intervals during the release. Figure 8 shows the measured (a) wind conditions, (b) CH_4 dry mole fraction, (c) release and IDM computed CH_4 flux. During the measurement, the downwind path altered between south beamline 1 and 2 as a function of time. The good comparison between the measured and calculated flux using both south beamlines demonstrated that altering the beam paths did not adversely impact our ability to determine a flux from the source area.

Formatted: Indent: First line: 0.3"

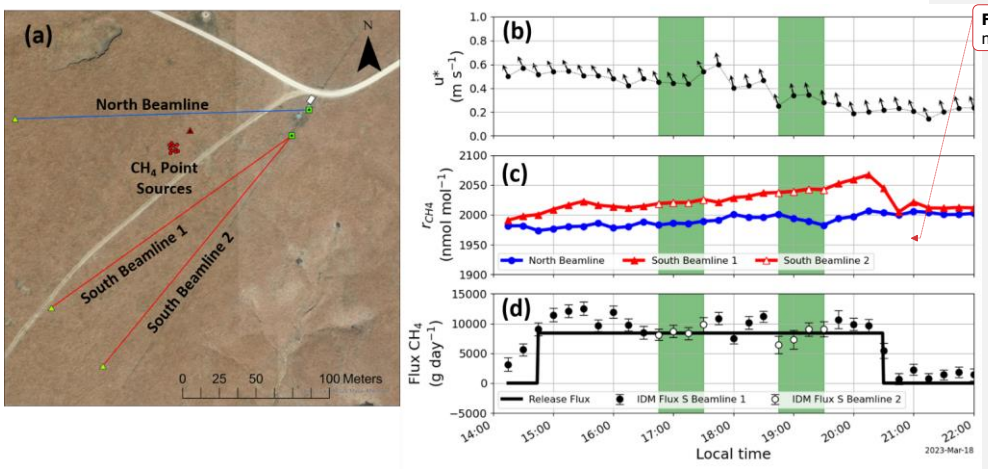

Formatted: Justified, Indent: Left: 0.3", No bullets or numbering

Figure 8: (a) Layout of the experimental site the Rannells' Flint Hills Prairie Preserve used to alternate between two downwind south paths. Timeseries of (b) wind friction velocity and direction, (c) CH_4 dry mole fraction, interferogram signal-to-noise, (d) release and IDM computed CH_4 flux for a release of 8396 g day^{-1}. The red triangle indicated the position of the 3D sonic anemometer. Wind arrows point in the direction from which the wind is blowing. The downwind South Beamline was changed during the release, focused on Retroreflector 2 at times 16:45 to 17:30, 18:45 to 19:30 (indicated by green shaded regions), and at Retroreflector 1 at all other times. Moving between the two downwind paths did not distort the concentration measurement or the computed IDM flux compared to the release rate.

94 Future work and conclusions

The agreement between the computed and actual CH_4 fluxes in this study shows that DCS can precisely measure the small CH_4 concentration enhancements due to a herd of beef cattle in the field at distances up to 100 m from the source area. Our ability to measure results show that the DCS precision is limited to the ability to maintain sufficient laser alignment between transceiver and retroreflector. A robust transceiver design and housing, along with a fast response datalogger-controlled gimbal alignment is critical to make continuous measurements under turbulent and varying environmental conditions.

In addition to the good precision, other important characteristics of the DCS measurement were highlighted in this study: 1) the use of inexpensive (US$1.3 per meter) and robust telecommunication-grade fibre optics (SMF28) to transport the light from the DCS to outdoor transceivers over long distances (tens to hundreds of meters) with very low power losses (4.5% loss per km) and 2) its ability to measure multiple open atmospheric laser beamlines simultaneously with a single instrument. From a pure measurement standpoint, using a single instrument to measure gradients of concentration is desirable to eliminate measurement biases. For example, cross calibrations are often necessary when using multiple line average sensors to perform multi-path gas concentration measurements. The minimization of instrument biases is crucial when combining the DCS with

existing micrometeorological techniques that utilize of vertical or horizontal gradients of concentration to infer fluxes (Flesch et al., 1995; McGinn and Flesch, 2018a). Expected CH_4 horizontal gradients in grazing systems are often small, as demonstrated in this study, so small instrument biases can lead to large errors when inferring fluxes. Furthermore, the use of a single instrument to measure multiple source areas will also lead to a reduction of the cost necessary to evaluate multiple treatments. This is particularly important when assessing GHG mitigation strategies, which often require evaluation of multiple treatments and management practices simultaneously.

The driving rationale of this work is to quantify the net CH_4 fluxes produced by cattle grazing system, which will require measuring wind velocity and CH_4 concentration enhancements upwind and downwind of the animals over long times. Although soil CH_4 fluxes are expected to be smaller than animal emissions, they could be important for estimating whole-system CH_4 budgets. Separating animal and soil contributions to the net CH_4 fluxes will require a combination of measuring approaches, such as chamber and micrometeorological measurements (*e.g.* eddy covariance measurements). High animal mobility in extensive grazing systems will also pose additional challenges for the quantification of cattle emissions. The ability to track cattle for laser-based greenhouse gas detection is an open and significant problem. Animal tracking using GPS collars (Felber et al., 2015) or digital photographs (Stoy et al., 2021) have been used to track ruminants in grazing systems. Both approaches have their own challenges, GPS collars need to provide high accuracy and temporal resolution spatial data while consuming low power to allow animals to be monitored during an entire grazing season. Wide-angle camera images were used to determine the position of the cattle herd during Summer 2023 with limited success (data not shown), since it was difficult to properly discern animal positions with enough spatial resolution needed for the IDM. Ideally, real-time animal tracking using GPS collars, digital images or a combination of both could be used to improve flux estimate accuracies. This could be done by subdividing the grazing system into small monitoring areas. The area monitored by the DCS system could be selected by aiming the laser beam at different retroreflectors installed at different points of the pasture. By monitoring these small areas, it would be possible to keep the downwind laser beam close to the animals, thus, measuring a larger CH_4 concentration enhancement and reducing the uncertainties in concentration measurements. The ability of DCS to measure gases from a large area continuously will permit monitoring of CH_4 emissions from a slow-moving herd of cattle, providing precise CH_4 flux values to improve agricultural GHG inventories and management practices.

~~10~~5 Author contribution

I.C., B.D.D, K.C.C, S.M.W., C.B, C.E.O, N.R.N., E.A.S., and B.R.W. conceived of and designed the experiments. E.A.S., D.I.H., N.A.M and B.R.W. built the DCS system. F.R.G and B.R.W wrote DCS data acquisition code. N.A.M and B.R.W. wrote the spectral line fitting code. C.W., L.C.M., E.A.S., and B.R.W. performed the experiments and analysed the data. C.E.O is the manager of the Rannells' Ranch. L.C.M., C. W., K.C.C., E.A.S., and B.R.W. performed the experiments and analyzed

the DCS data. C.W. and E.A.S. implemented the inverse dispersion model. B.R.W. and E.A.S. supervised the project. All authors contributed to the writing of this manuscript.

~~11~~6 Competing interests

The authors declare that they have no competing interests.

~~12~~7 Data and materials availability

Data associated with this paper is publicly available at https://doi.org/10.18434/mds2-3139 or can be obtained from the authors upon a reasonable request.

~~13~~8 Acknowledgements

This work was partially funded by the NSF Division of Biological Infrastructure Award #1726304, the William and Joan Porter Endowment, the Habiger Heritage Fund, and NIST.

~~14~~9 References

Alden, C. B., Coburn, S. C., Wright, R. J., Baumann, E., Cossel, K., Perez, E., Hoenig, E., Prasad, K., Coddington, I., and Rieker, G. B.: Single-Blind Quantification of Natural Gas Leaks from 1 km Distance Using Frequency Combs, Environ. Sci. Technol., 53, 2908–2917, https://doi.org/10.1021/acs.est.8b06259, 2019.

Alemu, A. W., Janzen, H., Little, S., Hao, X., Thompson, D. J., Baron, V., Iwaasa, A., Beauchemin, K. A., and Kröbel, R.: Assessment of grazing management on farm greenhouse gas intensity of beef production systems in the Canadian Prairies using life cycle assessment, Agricultural Systems, 158, 1–13, https://doi.org/10.1016/j.agsy.2017.08.003, 2017.

Bai, M., Loh, Z., Griffith, D. W. T., Turner, D., Eckard, R., Edis, R., Denmead, O. T., Bryant, G. W., Paton-Walsh, C., Tonini, M., McGinn, S. M., and Chen, D.: Performance of open-path lasers and Fourier transform infrared spectroscopic systems in agriculture emissions research, Atmospheric Measurement Techniques, 15, 3593–3610, https://doi.org/10.5194/amt-15-3593-2022, 2022.

Coates, T. W., Flesch, T. K., McGinn, S. M., Charmley, E., and Chen, D.: Evaluating an eddy covariance technique to estimate point-source emissions and its potential application to grazing cattle, Agricultural and Forest Meteorology, 234, 164–171, 2017.

Coburn, S., Alden, C. B., Wright, R., Cossel, K., Baumann, E., Truong, G.-W., Giorgetta, F., Sweeney, C., Newbury, N. R., Prasad, K., Coddington, I., and Rieker, G. B.: Regional trace-gas source attribution using a field-deployed dual frequency comb spectrometer, Optica, 5, 320–327, https://doi.org/10.1364/OPTICA.5.000320, 2018.

Coddington, I., Newbury, N., and Swann, W.: Dual-comb spectroscopy, Optica, 3, 414–426, https://doi.org/10.1364/OPTICA.3.000414, 2016.

Cole, R. K., Makowiecki, A. S., Hoghooghi, N., and Rieker, G. B.: Baseline-free quantitative absorption spectroscopy based on cepstral analysis, Opt. Express, 27, 37920, https://doi.org/10.1364/OE.27.037920, 2019.

Crenna, B.: An introduction to WindTrax, University of Alberta, 2006, http://thunderbeachscientific.com/downloads/introduction.pdf.

Danielsson, R., Ramin, M., Bertilsson, J., Lund, P., and Huhtanen, P.: Evaluation of a gas in vitro system for predicting methane production in vivo, Journal of dairy science, 100, 8881–8894, 2017.

Dengel, S., Levy, P. E., Grace, J., Jones, S. K., and Skiba, U. M.: Methane emissions from sheep pasture, measured with an open-path eddy covariance system, Global Change Biology, 17, 3524–3533, https://doi.org/10.1111/j.1365-2486.2011.02466.x, 2011.

Eggleston, S., Buendia, L., Miwa, K., Mgara, T., and Tanabe, K.: Emissions from Livestock and Manure Management, in: 2006 IPCC Guidelines for National Greenhouse Gas Inventories, vol. 4, Institute for Global Environmental Strategies, 2006.

EPA: Inventory of U.S. greenhouse gas emissions and sinks:1990-2021., 2023.

Felber, R., Münger, A., Neftel, A., and Ammann, C.: Eddy covariance methane flux measurements over a grazed pasture: effect of cows as moving point sources, Biogeosciences, 12, 3925–3940, https://doi.org/10.5194/bg-12-3925-2015, 2015.

Flesch, T., Wilson, J., Harper, L., and Crenna, B.: Estimating gas emissions from a farm with an inverse-dispersion technique, Atmospheric Environment, 39, 4863–4874, https://doi.org/10.1016/j.atmosenv.2005.04.032, 2005.

Flesch, T. K., Wilson, J. D., and Yee, E.: Backward-time Lagrangian stochastic dispersion models and their application to estimate gaseous emissions, Journal of Applied Meteorology and Climatology, 34, 1320–1332, 1995.

Flesch, T. K., Wilson, J. D., Harper, L. A., Crenna, B. P., and Sharpe, R. R.: Deducing Ground-to-Air Emissions from Observed Trace Gas Concentrations: A Field Trial, JOURNAL OF APPLIED METEOROLOGY, 43, 16, 2004.

Flesch, T. K., Basarab, J. A., Baron, V. S., Wilson, J. D., Hu, N., Tomkins, N. W., and Ohama, A. J.: Methane emissions from cattle grazing under diverse conditions: An examination of field configurations appropriate for line-averaging sensors, Agricultural and Forest Meteorology, 258, 8–17, https://doi.org/10.1016/j.agrformet.2017.10.012, 2018.

Gordon, I. E., Rothman, L. S., Hill, C., Kochanov, R. V., Tan, Y., Bernath, P. F., Birk, M., Boudon, V., Campargue, A., Chance, K. V., Drouin, B. J., Flaud, J.-M., Gamache, R. R., Hodges, J. T., Jacquemart, D., Perevalov, V. I., Perrin, A., Shine, K. P., Smith, M.-A. H., Tennyson, J., Toon, G. C., Tran, H., Tyuterev, V. G., Barbe, A., Császár, A. G., Devi, V. M., Furtenbacher, T., Harrison, J. J., Hartmann, J.-M., Jolly, A., Johnson, T. J., Karman, T., Kleiner, I., Kyuberis, A. A., Loos, J., Lyulin, O. M., Massie, S. T., Mikhailenko, S. N., Moazzen-Ahmadi, N., Müller, H. S. P., Naumenko, O. V., Nikitin, A. V., Polyansky, O. L., Rey, M., Rotger, M., Sharpe, S. W., Sung, K., Starikova, E., Tashkun, S. A., Auwera, J. V., Wagner, G., Wilzewski, J., Wcisło, P., Yu, S., and Zak, E. J.: The HITRAN2016 molecular spectroscopic database, Journal of Quantitative Spectroscopy and Radiative Transfer, 203, 3–69, https://doi.org/10.1016/j.jqsrt.2017.06.038, 2017.

Grainger, C., Clarke, T., McGinn, S. M., Auldist, M. J., Beauchemin, K. A., Hannah, M. C., Waghorn, G. C., Clark, H., and Eckard, R. J.: Methane emissions from dairy cows measured using the sulfur hexafluoride (SF6) tracer and chamber techniques, Journal of Dairy Science, 90, 2755–2766, https://doi.org/10.3168/jds.2006-697, 2007.

Griffiths, P. and de Haseth, J.: Fourier Transform Infrared Spectrometry, John Wiley & Sons, Inc, 2006.

Formatted: Left

Harper, L. A., Flesch, T. K., Weaver, K. H., and Wilson, J. D.: The Effect of Biofuel Production on Swine Farm Methane and Ammonia Emissions, J of Env Quality, 39, 1984–1992, https://doi.org/10.2134/jeq2010.0172, 2010.

Herman, D. I., Weerasekara, C., Hutcherson, L. C., Giorgetta, F. R., Cossel, K. C., Waxman, E. M., Colacion, G. M., Newbury, N. R., Welch, S. M., DePaola, B. D., Coddington, I., Santos, E. A., and Washburn, B. R.: Precise multispecies agricultural gas flux determined using broadband open-path dual-comb spectroscopy, Sci Adv, 7, eabe9765, https://doi.org/10.1126/sciadv.abe9765, 2021.

Hill, J., McSweeney, C., Wright, A.-D. G., Bishop-Hurley, G., and Kalantar-zadeh, K.: Measuring methane production from ruminants, Trends in biotechnology, 34, 26–35, 2016.

Hristov, A. N., Oh, J., Giallongo, F., Frederick, T., Weeks, H., Zimmerman, P. R., Harper, M. T., Hristova, R. A., Zimmerman, R. S., and Branco, A. F.: The Use of an Automated System (GreenFeed) to Monitor Enteric Methane and Carbon Dioxide Emissions from Ruminant Animals, JoVE, 52904, https://doi.org/10.3791/52904, 2015.

Johnson, K., Huyler, M., Westberg, H., Lamb, B., and Zimmerman, P.: Measurement of methane emissions from ruminant livestock using a sulfur hexafluoride tracer technique, Environmental science & technology, 28, 359–362, 1994.

Kochanov, R. V., Gordon, I. E., Rothman, L. S., Wcisło, P., Hill, C., and Wilzewski, J. S.: HITRAN Application Programming Interface (HAPI): A comprehensive approach to working with spectroscopic data, Journal of Quantitative Spectroscopy and Radiative Transfer, 177, 15–30, https://doi.org/10.1016/j.jqsrt.2016.03.005, 2016.

Laubach, J. and Kelliher, F. M.: Methane emissions from dairy cows: Comparing open-path laser measurements to profile-based techniques, Agricultural and Forest Meteorology, 135, 340–345, https://doi.org/10.1016/j.agrformet.2005.11.014, 2005.

Laubach, J., Barthel, M., Fraser, A., Hunt, J. E., and Griffith, D. W. T.: Combining two complementary micrometeorological methods to measure CH_4 and N_2O fluxes over pasture, Biogeosciences, 13, 1309–1327, https://doi.org/10.5194/bg-13-1309-2016, 2016.

Laubach, J., Flesch, T. K., Ammann, C., Bai, M., Gao, Z., Merbold, L., Campbell, D. I., Goodrich, J. P., Graham, S. L., Hunt, J. E., Wall, A. M., and Schipper, L. A.: Methane emissions from animal agriculture: Micrometeorological solutions for challenging measurement situations, Agricultural and Forest Meteorology, 350, 109971, https://doi.org/10.1016/j.agrformet.2024.109971, 2024.

Lockyer, D. and Jarvis, S.: The measurement of methane losses from grazing animals, Environmental Pollution, 90, 383–390, 1995.

Malarich, N. A., Cossel, K. C., Deschenes, J.-D., Giorgetta, F. R., Washburn, B. R., Newbury, N. R., Genest, J., and Coddington, I.: Removing biases in dual frequency comb spectroscopy due to digitizer nonlinearity, Opt. Express, 31, 29074, https://doi.org/10.1364/OE.497497, 2023.

McGinn, S. and Flesch, T.: A Technique for Estimating Greenhouse Gas Exchange Adjacent Cattle Feedlots, Atmosphere, 9, 139, https://doi.org/10.3390/atmos9040139, 2018a.

McGinn, S. M.: Developments in micrometeorological methods for methane measurements, animal, 7, 386–393, https://doi.org/10.1017/S1751731113000657, 2013.

McGinn, S. M. and Flesch, T. K.: Ammonia and greenhouse gas emissions at beef cattle feedlots in Alberta Canada, Agricultural and Forest Meteorology, 258, 43–49, https://doi.org/10.1016/j.agrformet.2018.01.024, 2018b.

McGinn, S. M., Turner, D., Tomkins, N., Charmley, E., Bishop-Hurley, G., and Chen, D.: Methane Emissions from Grazing Cattle Using Point-Source Dispersion, J. Environ. Qual., 40, 22–27, https://doi.org/10.2134/jeq2010.0239, 2011.

Newville, M., Stensitzki, T., Allen, D., and Ingargiola, A.: LMFIT: Non-Linear Least-Square Minimization and Curve-Fitting for Python, 2014 https://dx.doi.org/10.5281/zenodo.11813.

Phillips, F., Leuning, R., Baigent, R., Kelly, K., and Denmead, O.: Nitrous oxide flux measurements from an intensively managed irrigated pasture using micrometeorological techniques, Agricultural and Forest Meteorology, 143, 92–105, 2007.

Pinares-Patiño, C., Lassey, K., Martin, R., Molano, G., Fernandez, M., MacLean, S., Sandoval, E., Luo, D., and Clark, H.: Assessment of the sulphur hexafluoride (SF6) tracer technique using respiration chambers for estimation of methane emissions from sheep, Animal feed science and technology, 166, 201–209, 2011.

Place, S. E., Pan, Y., Zhao, Y., and Mitloehner, F. M.: Construction and operation of a ventilated hood system for measuring greenhouse gas and volatile organic compound emissions from cattle, Animals, 1, 433–446, 2011.

Prajapati, P. and Santos, E. A.: Comparing methane emissions estimated using a backward-Lagrangian stochastic model and the eddy covariance technique in a beef cattle feedlot, Agricultural and Forest Meteorology, 256–257, 482–491, https://doi.org/10.1016/j.agrformet.2018.04.003, 2018a.

Prajapati, P. and Santos, E. A.: Estimating methane emissions from beef cattle in a feedlot using the eddy covariance technique and footprint analysis, Agricultural and Forest Meteorology, 258, 18–28, https://doi.org/10.1016/j.agrformet.2017.08.004, 2018b.

Ramin, M. and Huhtanen, P.: Development of equations for predicting methane emissions from ruminants, Journal of Dairy Science, 96, 2476–2493, 2013.

Rothman, L. S., Gordon, I. E., Barbe, A., Benner, D. C., Bernath, P. E., Birk, M., Boudon, V., Brown, L. R., Campargue, A., Champion, J. P., Chance, K., Coudert, L. H., Dana, V., Devi, V. M., Fally, S., Flaud, J. M., Gamache, R. R., Goldman, A., Jacquemart, D., Kleiner, I., Lacome, N., Lafferty, W. J., Mandin, J. Y., Massie, S. T., Mikhailenko, S. N., Miller, C. E., Moazzen-Ahmadi, N., Naumenko, O. V., Nikitin, A. V., Orphal, J., Perevalov, V. I., Perrin, A., Predoi-Cross, A., Rinsland, C. P., Rotger, M., Simeckova, M., Smith, M. A. H., Sung, K., Tashkun, S. A., Tennyson, J., Toth, R. A., Vandaele, A. C., and Vander Auwera, J.: The HITRAN 2008 molecular spectroscopic database, J. Quant. Spectrosc.Radiat. Transfer, 110, 533–572, https://doi.org/10.1016/j.jqsrt.2009.02.013, 2009.

Rothman, L. S., Gordon, I. E., Babikov, Y., Barbe, A., Chris Benner, D., Bernath, P. F., Birk, M., Bizzocchi, L., Boudon, V., Brown, L. R., Campargue, A., Chance, K., Cohen, E. A., Coudert, L. H., Devi, V. M., Drouin, B. J., Fayt, A., Flaud, J.-M., Gamache, R. R., Harrison, J. J., Hartmann, J.-M., Hill, C., Hodges, J. T., Jacquemart, D., Jolly, A., Lamouroux, J., Le Roy, R. J., Li, G., Long, D. A., Lyulin, O. M., Mackie, C. J., Massie, S. T., Mikhailenko, S., Müller, H. S. P., Naumenko, O. V., Nikitin, A. V., Orphal, J., Perevalov, V., Perrin, A., Polovtseva, E. R., Richard, C., Smith, M. A. H., Starikova, E., Sung, K., Tashkun, S., Tennyson, J., Toon, G. C., Tyuterev, Vl. G., and Wagner, G.: The HITRAN 2012 molecular spectroscopic database, J. Quant. Spectrosc.Radiat. Transfer, 130, 4–50, https://doi.org/10.1016/j.jqsrt.2013.07.002, 2013.

Rotz, C. A., Asem-Hiablie, S., Dillon, J., and Bonifacio, H.: Cradle-to-farm gate environmental footprints of beef cattle production in Kansas, Oklahoma, and Texas, Journal of Animal Science, 93, 2509–2519, https://doi.org/10.2527/jas.2014-8809, 2015.

Sinclair, L. C., Deschênes, J.-D., Sonderhouse, L., Swann, W. C., Khader, I. H., Baumann, E., Newbury, N. R., and Coddington, I.: Invited Article: A compact optically coherent fiber frequency comb, Review of Scientific Instruments, 86, 081301, https://doi.org/10.1063/1.4928163, 2015.

Smith, E. F. and Owensby, C. E.: Intensive-Early Stocking and Season-Long Stocking of Kansas Flint Hills Range, Journal of Range Management, 31, 14, https://doi.org/10.2307/3897624, 1978.

Storm, I. M. L. D., Hellwing, A. L. F., Nielsen, N. I., and Madsen, J.: Methods for measuring and estimating methane emission from ruminants, Animals, 2, 160–183, https://doi.org/10.3390/ani2020160, 2012.

Stoy, P. C., Cook, A. A., Dore, J. E., Kljun, N., Kleindl, W., Brookshire, E. N. J., and Gerken, T.: Methane efflux from an American bison herd, Biogeosciences, 18, 961–975, https://doi.org/10.5194/bg-18-961-2021, 2021.

Sun, K., Tao, L., Miller, D. J., Zondlo, M. A., Shonkwiler, K. B., Nash, C., and Ham, J. M.: Open-path eddy covariance measurements of ammonia fluxes from a beef cattle feedlot, Agricultural and Forest Meteorology, 213, 193–202, https://doi.org/10.1016/j.agrformet.2015.06.007, 2015.

Thompson, L. R. and Rowntree, J. E.: Invited Review: Methane sources, quantification, and mitigation in grazing beef systems, Applied Animal Science, 36, 556–573, https://doi.org/10.15232/aas.2019-01951, 2020.

Todd, R. W., Altman, M. B., Cole, N. A., and Waldrip, H. M.: Methane Emissions from a Beef Cattle Feedyard during Winter and Summer on the Southern High Plains of Texas, Journal of Environmental Quality, 43, 1125–1130, https://doi.org/10.2134/jeq2013.09.0386, 2014.

Truong, G.-W., Waxman, E. M., Cossel, K. C., Baumann, E., Klose, A., Giorgetta, F. R., Swann, W. C., Newbury, N. R., and Coddington, I.: Accurate frequency referencing for fieldable dual-comb spectroscopy, Optics Express, 24, 30495–30504, https://doi.org/10.1364/OE.24.030495, 2016.

Werle, P.: Accuracy and precision of laser spectrometers for trace gas sensing in the presence of optical fringes and atmospheric turbulence, Appl. Phys. B, 102, 313–329, https://doi.org/10.1007/s00340-010-4165-9, 2011.